IMEKO 2010 TC3, TC5 and TC22 Conferences
Metrology in Modern Context
November 22–25, 2010, Pattaya, Chonburi, Thailand

3-D SURFACE ROUGHNESS PROFILE OF 316-STAINLESS STEEL USING VERTICAL SCANNING INTERFEROMETRY WITH A SUPERLUMINESCENT DIODE

Wirun Laopornpichayanuwat[1], *Jakkapol Visessamit*[2], *Montian Tianprateep*[3]

[1]National Institute of Metrology (Thailand), Pathumthani, Thailand, wirun@nimt.or.th
[2&3]Faculty of Science, Chulalongkorn University, Bangkok, Thailand, Montian.T@chula.ac.th

Abstract – Surface roughness is one of many parameters that influences on mass stability of standard weight, commonly used as a transfer standard of mass SI unit. One of the most famous non-invasive methods for determining surface roughness from a surface profile of material is a vertical scanning interferometry (VSI) with a white light source. In this research, 3-D surface profiles of 316-stainless steel, usually used as a material for standard weights, are constructed by using VSI, based on Michelson interferometer (MI). Because of its low-coherent properties, low cost, and compact light source, a superluminescent diode (SLD) is chosen as a low-coherence light source in our interferometry system. Since a continuous wavelet transform (CWT) algorithm provides accuracy results, it is also used as a numerical analyzing method for the interferogram signals, taking from our VSI. The surface roughness and measurement uncertainty, calculated from the constructed 3-D surface roughness profiles of 316-stainless steel samples, are discussed.

Keywords: Roughness, Vertical scanning interferometry (VSI), Continuous wavelet transform (CWT)

1. INTRODUCTION

Optical interferometry is a popular noncontact measurement technique, used for constructing a high resolution 3-D surface profile[1]. Recently, an optical coherence tomography (OCT), based on vertical scanning interferometry (VSI) with a low-coherent light source, is one of the most famous non-invasive and non-contact method for determining the microscopic properties, such as thickness, roughness, and surface profile, of materials, detecting subsurface deflection area, and constructing a cross-section image of both living tissue and non-living substance sample[2,3,4].

Because of its coherence length, which is only a few micrometer scales, the low-coherence light source is a key of OCT's success. Two low-coherent light sources, widely used in OCT, are halogen lamp and superluminescent diode (SLD)[5,6]. Although, the halogen lamp produces a high intensity light, it has a large size and produces more heat. So, the SLD is more suitable for using in a compact measuring system than the halogen lamp, because of its compact size and less heat production. It is also not expensive. However, because the SLD is a low intensity light source, a sample having poor reflected surface, is almost impossible to measuring without consuming time. A conservative way to construct this kind of sample is gradually moving both x-, y- and z- axis of a reference mirror in the interferometer system.

With the halogen light source, VSI, that beam of light source was set as a parallel beam and CCD camera was applied as a detector of the system, could decrease constructing time[7]. With this method, the beam is approximated as a set of a small light source. Thus, the intensity, detected in each pixel of the CCD camera, is represented as the intensity of the small light source, reflected from each point of the sample surface. Because surface roughness of a standard weight, commonly used as a transfer standard of mass SI unit and made from 316-stainless steel, is very low, it almost reflect all of incident light, even through those light is came from a low intensity light source, such as, SLD. Therefore, the possibility of constructing 3-D profiles of two well polished 316-stainless steel surfaces by setting SLD to be parallel beam and using CCD camera as a detector in VSI, will be confirmed in this research.

One important thing for 3-D surface profile construction is a method for analyzing the interferogram signal. As a continuous wavelet transform (CWT) provided an accuracy result for VSI with halogen light source[8], CWT will also used as analytical tools for constructing 3-D surface profiles of our samples.

2. TECHNICAL DETAILS

The concept of a VSI system, used in this research, is seen in Fig.1. A parallel beam from a SLD light source propagates through a beamsplitter (BS) and is divided into two beams. One, called sample arm goes straight to a sample, another, called reference arm, goes straight to a reference mirror. The reflected sample and reference arms are recombined at BS to produce an interference fringe pattern, detected by CCD camera. By fixing the sample and moving the reference mirror in z-direction, each pixel of CCD can detect the intensity, depending on z-position of reference arm as;

$$I(z) = I_0\left\{1+V\exp\left[-\left(\frac{z-z_0}{l_C}\right)^2\right]\cos\left(4\pi\frac{z-z_0}{\lambda_0}\right)\right\}, \quad (1)$$

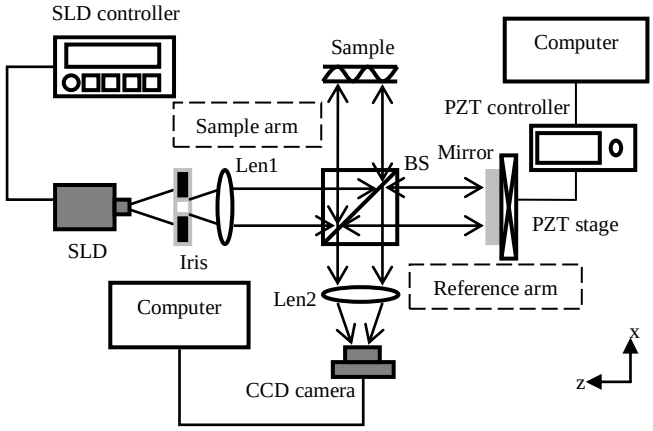

Fig. 1. Schematic of experimental setup.

where I_0 is the background intensity, V is the visibility, z is the vertical scanning position along the optical axis, z_0 is the zero-order fringe position, l_C is the coherence length of a light source, and λ_0 is the central wavelength of a light source.

In order to analyze the interferogram that consists of the discrete signals, CWT is scoped to use in this research. The result, getting from CWT, will lead to find an actual position, having the maximum intensity. Because the interferogram has a Gaussian shape, the Morlet wavelet, having a plane wave modulated by a Gaussian, is chosen as a mother wavelet in this research. It is expressed by [9]

$$h(\eta) = \left[\exp(i\omega_0\eta) - \exp\left(-\frac{\omega_0^2}{2}\right) \right] \exp\left(-\frac{\eta^2}{2}\right) \qquad (2)$$

where η is a nondimensional time parameter and ω_0 is the nondimensional frequency [10].

For the interferogram with the discrete signals in z direction, the wavelet transform function becomes [10]

$$W_{a,b}(z) = \sqrt{\frac{\Delta z}{|a|}} \sum_{z=0}^{N-1} I(z) h^* \left[\left(\frac{z-b}{a} \right) \Delta z \right] \qquad (3)$$

where $h^*(z)$ is the complex conjugation of mother wavelet from (2) by replacing η with z, a is a scale parameter (compression or expansion the mother wavelet), b is a translation parameter, Δz is an increasing step, and N is a number of signals.

Due to the discrete signals of the interferogram, an actual peak may place between an experimental peak and an adjacent point, as shown in Fig. 2. By using CWT, a phase of each peak can be used to calculate the distance between the experimental peak and the actual peak. Because the wavelet transform function $W_{a,b}(z)$ consists of real part and imaginary part, the phase φ of the wavelet transform can be calculated by

$$\varphi = \tan^{-1}\left(\frac{\mathrm{Im}\{W_{a\_\max, b\_\max}(z)\}}{\mathrm{Re}\{W_{a\_\max, b\_\max}(z)\}} \right) \qquad (4)$$

where a_max and b_max are a position that the amplitude $|W_{a,b}(z)|$ has a maximum value.

Thus, a relation of the actual peak and the experimental peak can be written as [7]

$$z_R = z_M - \frac{\lambda_0}{4\pi}\varphi \qquad (5)$$

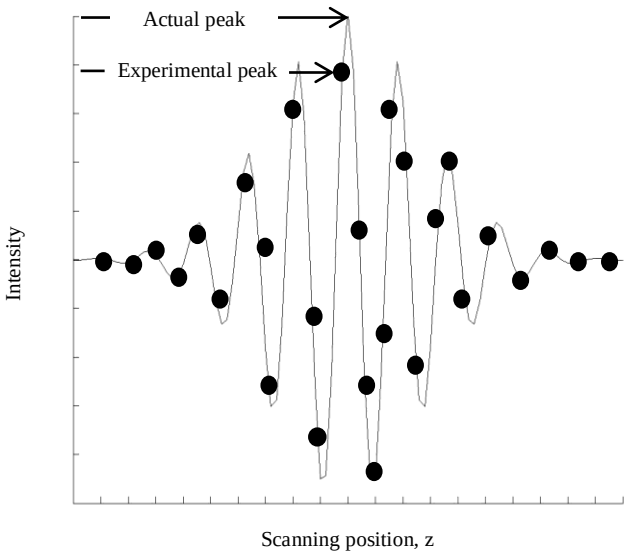

Fig. 2. Definition of actual peak and experiment peak of interferogram

where z_R is a real maximum position, z_M is a maximum position, φ is a phase of the maximum position from a wavelet analysis.

3. MEASUREMENT

In this research, the Michelson interferometer and the SLD were used to characterize the surface profile of samples. Two circular shape plates of stainless steel with a diameter of 25 mm were used as samples. These samples were well polished to make a good reflect of light. The experimental system was arranged as shown in Fig. 1. The SLD generated a light beam, collimated by len 1 to become a parallel beam. Then, this light beam was split into two arms; a reference arm and a sample arm, by BS. Each beam reflected from the end of each arm, combined together and traveled to len 2, and was detected by a 640×480 pixels SONY XCD-V50CR CCD camera. Because this combination beam contained path differences between two arms, thus, the interference patterns could be observed. As the parallel beam can be assumed as an array of small light sources, each CCD pixel also can detect the interferogram of a small area of the sample surface.

For recording the interferogram, a reference mirror, mounted on the PZT stage at the end of reference arm, was gradually moved along the z-direction by computer controlling. Because a central wavelength of the SLD was 830 nm, a step of PZT stage was chosen as 100 nm (0.1 μm) in order to obey the sampling theorem. A series of intensity signals, detected by each pixel of CCD, in every step produced an individual interferogram. The example of interferogram, collected by one pixel of CCD, shows in Fig. 3. Then, CWT was applied to that interferogram for defining its actual peak, represented as a height of the surface at that pixel area. The CWT spectrogram of interferogram, shown in Fig. 3, is represented in Fig. 4. By combining the results calculated from every pixels of CCD, 3-D surface profile could be constructed.

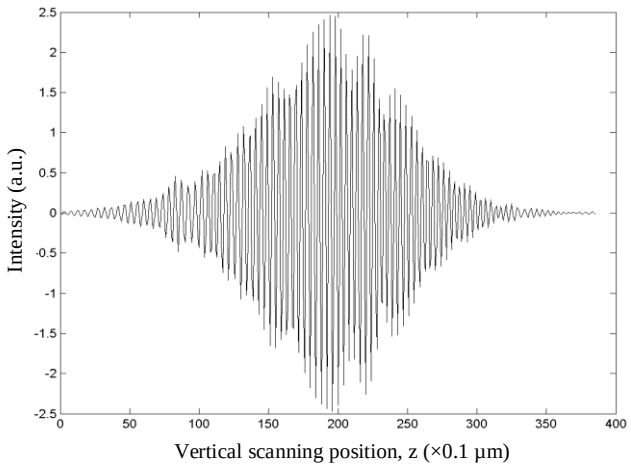

Fig. 3. An example of intensity signals in each vertical scanning step of one pixel.

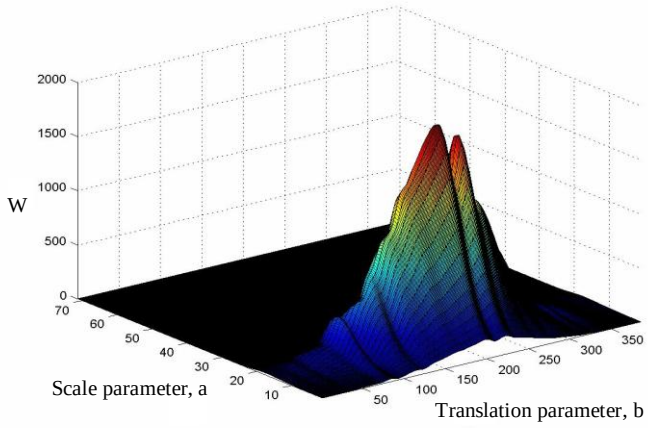

Fig. 4. CWT spectrogram of intensity signal shown in Fig. 3

4. RESULTS AND DISCUSSIONS

The mean height of roughness (R_a), root-mean-square height of roughness (R_q), and maximum height of roughness (R_z) of two stainless steel plates were calculated by using the light beam, recorded by CCD camera. Light beam, used in this research, had a size of 4 × 3 mm in x-axis and y-axis, respectively. Since the CCD camera had 640 x-axis pixels and 480 y-axis pixels; therefore, each pixel of the CCD camera represented 6.25 × 6.25 µm image sizes. To avoid flare light, which reflected from neighbour CCD pixels, an average of 4 × 4 pixels would be considered as a surface area. Thus, the whole image had 160 × 120 values and each value contained an area size of 25 × 25 µm. In this research, a cross-section of each stainless steel sample was measured from 101st-104th (line 1), 201st-204th (line2), 301st-304th (line 3) and 401st-404th (line 4) y-axis pixels, as shown in Fig. 5a and 5b respectively.

After applied CWT method with the interferogram of every sampling area of CCD camera, a set of maximum $W_{a\_\max,b\_\max}(z)$ of the CWT spectrogram and real position of surface height, z_R could be calculated by (5). Then, 3-D surface roughness profile of two stainless steel plates could be constructed from all z_R.

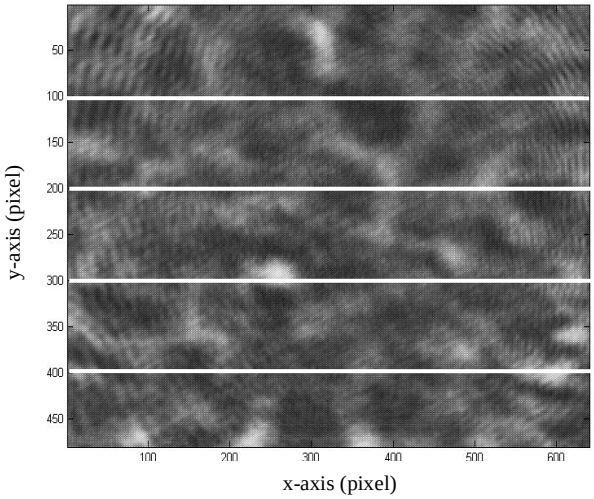

Fig. 5a. Selection lines for constructing cross-section and surface image of Sample No.1

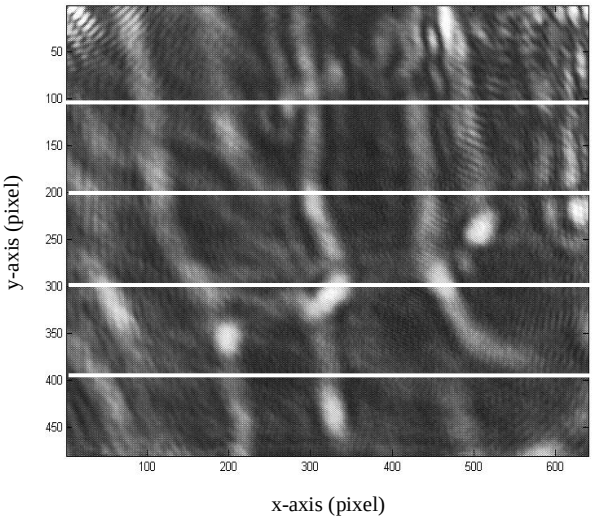

Fig. 5b. Selection lines for constructing cross-section and surface image of Sample No.2

The example of 3-D surface roughness profile of 500×500 µm area for each 316-stainless steel plate (Sample No. 1 and No. 2) are shown in Fig. 6a and 6b, respectively.

From the experimentally obtained the mean height of roughness (R_a), root-mean-square height of roughness (R_q), and maximum height of roughness (R_z) of 316-stainless steel is averaged from 4 lines.

In this experiment, the measurement uncertainty is calculated according to M3003 [11], the source of uncertainty of a system, as shown in Table 1.

Table 1. Source of uncertainty

Source of uncertainty	c_i	$u(x_i)$
Repeatability (u_A)	1	$SD/\sqrt{n}$
Wavelength bandwidth ($u_{\Delta\lambda}$)	$\pi/4\pi$	$\Delta\lambda/\sqrt{3}$
Error of the PZT (u_{PZT})	1	$error\ of\ PZT\ /\sqrt{3}$
Roughness of reference mirror (u_R)	1	$roughness\ of\ reference\ mirror\ /\sqrt{3}$
Homogeneity of sample (u_{homo})	1	$(Max-Min)/\sqrt{3}$
Phase difference (u_φ)	$\lambda_0/4\pi$	$(Max-Min)/\sqrt{3}$

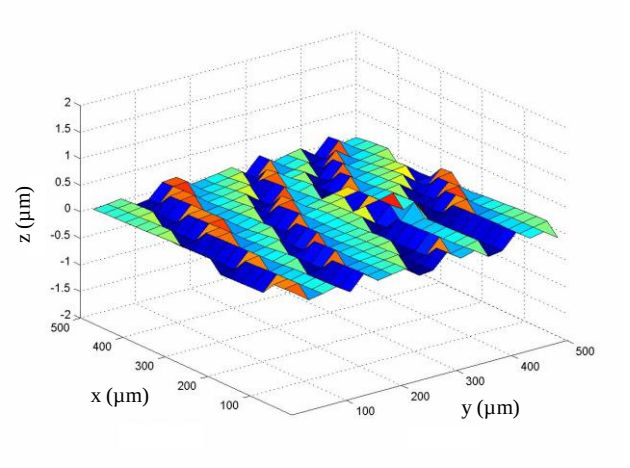

Fig. 6a. 3-D Surface roughness profile of Sample No.1

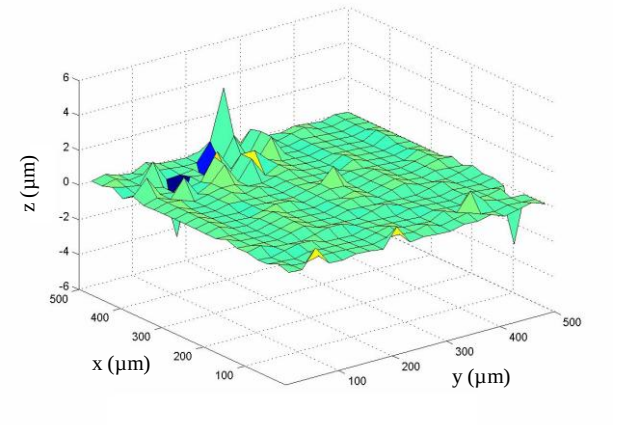

Fig. 6b. 3-D Surface roughness profile of Sample No.2

The uncertainty of a system is classified as types A and B. Type A uncertainty is obtained from a series of measurements on the repeatability of the system. Based on a series of measurements (n=10), type A uncertainty (u_A) due to random is less than 0.003 µm.

According to manufacture data, the wavelength bandwidth ($\Delta\lambda$) of SLD was 0.015 µm. So, assuming a rectangular distribution and based on (5), the distributed standard uncertainty was given by $u_{\Delta\lambda} = (0.015/\sqrt{3})(\pi/4\pi) = 0.002$ µm.

An error of the PZT stage could be compared with an input voltage that supply to this PZT stage. The maximum error in a distance, measured by manufacturer was 0.054 µm. The standard uncertainty using the rectangular distribution for this PZT stage was given by $u_{PZT} = 0.054/\sqrt{3} = 0.031$µm.

The mean height of roughness (R_a) of reference mirror, root-mean-square height of roughness (R_q) of reference mirror and maximum height of roughness (R_z) of reference mirror were 0.0005 µm, 0.0006 µm and 0.0014 µm respectively. The standard uncertainty of the reference mirror roughness using the rectangular distribution was given by $u_{Ra \text{ of mirror}} = 0.0003$ µm, $u_{Rq \text{ of mirror}} = 0.0003$ µm and $u_{Rz \text{ of mirror}} = 0.0008$ µm.

A homogeneity of each sample was different of surface roughness (Max-Min). The standard uncertainty of the homogeneity using the rectangular distribution was given by u_{homo} = (Max-Min)/$\sqrt{3}$ µm.

The phase difference has a type B uncertainty contributed by the algorithm. An ideal signal is given by

$$I(z) = 120 + 80\exp\left[-\left(\frac{z-z_0}{l_C}\right)^2\right]\cos\left(4\pi\frac{z-z_0}{\lambda_0}\right) \quad (6)$$

for z_0 = 20 µm, l_c = 20 µm and λ_0 = 830 nm (selected based on the natural characteristics of the illuminating light). Some prescribed phases are retrieved using CWT [7], the difference between maximum and minimum value of the phase difference is 0.0248 rad. Assuming a rectangular distribution and based on (5) the standard uncertainty is given by u_φ = [(0.0248)/$\sqrt{3}$]($\lambda_0/4\pi$) = 0.0009µm.

From the M3003 the expression of uncertainty and confidence in measurement, a combined uncertainty was given by

$$u_c = \sqrt{c_A^2u_A^2 + c_{\Delta\lambda}^2u_{\Delta\lambda}^2 + c_{PZT}^2u_{PZT}^2 + c_R^2u_R^2 + c_{homo}^2u_{homo}^2 + c_\varphi^2u_\varphi^2} \quad (7)$$

For a level of confidence of 95.5% with coverage factor k=2, an expanded uncertainty (U) of this system was expressed by

$$U = k \times u_c \quad (8)$$

The measurement uncertainty of surface roughness of 316-stainless steel samples, are listed in Table 2.

Table 2. The measurement uncertainty of surface roughness of samples

Source of uncertainty	Sample No.1			Sample No.2		
	R_a (µm)	R_q (µm)	R_z (µm)	R_a (µm)	R_q (µm)	R_z (µm)
u_A	0.0032	0.0032	0.0032	0.0032	0.0032	0.0032
$u_{\Delta\lambda}$	0.0022	0.0022	0.0022	0.0022	0.0022	0.0022
u_{PZT}	0.0312	0.0312	0.0312	0.0312	0.0312	0.0312
u_R	0.0003	0.0003	0.0008	0.0003	0.0003	0.0008
u_{homo}	0.0110	0.0104	0.0675	0.0040	0.0058	0.0635
u_φ	0.0009	0.0009	0.0009	0.0009	0.0009	0.0009
u_c	0.0333	0.0331	0.0745	0.0317	0.0320	0.0709
U	0.0666	0.0662	0.1490	0.0634	0.0639	0.1417

These samples were re-measured R_a, R_q and R_z by 3-D Non-Contact Surface Profiler SP-500 Series from Toray Engineering Co., Ltd. The light source is a halogen lamp. A comparison of roughness from SP-500 Series and this CWT method is shown in Table 3 and 4.

Table 3. Roughness of Sample No.1 from SP-500 Series and CWT

	SP-500		CWT		E_n
	Value	Uncertainty (k=2)	Value	Uncertainty (k=2)	
R_a	0.054 µm	0.013 µm	0.066 µm	0.067 µm	0.2
R_q	0.065 µm	0.015 µm	0.081 µm	0.066 µm	0.2
R_z	0.243 µm	0.069 µm	0.262 µm	0.149 µm	0.1

Table 4. Roughness of Sample No.2 from SP-500 Series and CWT

	SP-500		CWT		E_n
	Value	Uncertainty (k=2)	Value	Uncertainty (k=2)	
R_a	0.072 µm	0.016 µm	0.067 µm	0.063 µm	0.1
R_q	0.084 µm	0.018 µm	0.082 µm	0.064 µm	0.0
R_z	0.169 µm	0.049 µm	0.278 µm	0.142 µm	0.7

The E_n numbers is typically used in measurement comparison schemes, which is defined by [12]

$$E_n = \frac{x - X}{\sqrt{U_{lab}^2 + U_{ref}^2}} \qquad (9)$$

In this case, x is the value of CWT, X is the value of SP-500, U_{lab} is the expanded uncertainty of CWT and U_{ref} is the expanded uncertainty of SP-500. For E_n numbers, when $|E_n| \leq 1.0$ the result is satisfactory.

From Table 4, the E_n of R_z of Sample No.2 is nearly 1.0. Due to the measurement's results of SP-500 Series, light beam was focused to twenty small areas of sample surface. By comparing with CWT method, measuring area, covered by parallel beam, was 4 lines of 25 × 4000 µm, which was larger than the area, measured by SP-500 Series. In case the smooth surface sample, such as Sample No.1, the size of measuring area had no effect on R_z because values of surface roughness in almost every different area were close together. For Sample No.2, its surface was rougher than Sample No.1, then, the size of measuring size affected to its R_z. The smaller measuring area brought to smaller R_z than the larger one. Therefore, R_z, calculated from larger area, was suitable to represent the roughness of the whole sample surface.

5. CONCLUSIONS

This paper describes a method based on VSI for 3-D surface roughness profile measurement of 316-stainless steel. In addition, surface roughness of 316-stainless steel was measured by using a MI with SLD. Because of a micro-scale of SLD's coherence length and a VSI with CWT algorithm, an accuracy micro-scale of position in z-direction could be determined from a highest intensity position of interferogram. Two 316-stainless steel were tested by applying this VSI technique, and their surface roughness values were compared with ones measured from 3-D Non-Contact Surface Profiler SP-500 Series. According to the measuring results of these two samples, the calculated values of En numbers, which is an acceptable level based on ISO/IEC 17043[9], between surface roughness of these two methods were less than or equal to 1. In this research, it was found that the expanded uncertainty is depended on uncertainty from the error of the PZT stage and the homogeneity of sample. To reduce the dominant source of uncertainty, the expanded uncertainty will be decreased. The results suggest that this method can be applied to investigate the surface roughness of standard weight which more homogeneous than the sample.

ACKNOWLEDGEMENTS

This work was supported in part by Thailand Research Fund (Contact Number: MRG5280177)

REFERENCES

[1] N. Metchkarov, V. Sainov and P. Boone, "High-accuracy surface measurement using laser-diode phase-stepping interferometry", *Vacuum*, vol. 58, pp. 464-469, 2000.

[2] E. Jonathan, "Non-contact and non-destructive testing of silicon V-grooves: A non-medical application of optical coherence tomography (OCT)", *Optics and Lasers in Engineering*, vol.44, pp.1117-1131, 2006.

[3] M. D. Duncan and M. Bashkansky, "Subsurface defect detection in materials using optical coherence tomography", *Optics Express*, vol.2, no.13, pp.540-545, 1998.

[4] D. Huang, E. A. Swanson, C. P. Lin, J. S. Shuman, W. G. Stington, W. Chang, M. R. Hee, T. Flotte, K. Gregory, C. A. Puliafito and J. G. Fujimoto, "Optical Coherence Tomography", *Science*, vol. 254, no. 5035, pp. 1178-1181, 1991.

[5] P. Pavlíèek, "Height profile measurement by means of white light interferometry", *Proceedings of the SPIE*, vol. 5259, pp. 139-144, 2003.

[6] R. Onodera, H. Wakaumi and Y. Ishii, "Measurement technique for surface profiling in low-coherence interferometry", *Optics Communications*, vol. 254, pp. 52–57, 2005.

[7] M. Li, C. Quan and C. J. Tay, "Continuous wavelet transform for micro-component profile measurement using vertical scanning interferometry", *Optics & Laser Technology*, vol.40, pp.920-929, 2008.

[8] C. J. Tay, C. Quan and M. Li, "Investigation of a dual-layer structure using vertical scanning interferometry", Optics and Lasers in Engineering, vol. 45, pp. 907-913, 2007.

[9] L. Chongchun and Q. Zhengding, "A method based Morlet wavelet for extracting vibration signal envelope", *Proceedings of ICSP2000*, pp.337-340, 2000.

[10] C. Torrence and G. P. Compo, "A practice guide to wavelet analysis", *Bulletin of the American Meteorological Society*, vol.79, pp.61-78, 1998.

[11] United Kingdom Accreditation Service, "The Expression of Uncertainty and Confidence in Measurement", 2nd ed., London, 2007.

[12] ISO/IEC 17043, " Conformity assessment - General requirements for proficiency testing ", 2010.